ACI STRUCTURAL JOURNAL TECHNICAL PAPER

Title no. 95-S55

Pivot Hysteresis Model for Reinforced Concrete Members



by Robert K. Dowell, Frieder Seible, and Edward L. Wilson

For nonlinear dynamic seismic analysis of bridge structures to be practical, only the dominant nonlinear characteristics of the structure should be included. Based on capacity design principles, the current seismic bridge design philosophy is generally to force all member nonlinearities into the ends of ductile columns. Therefore, nonlinear characteristics of the columns must be adequately defined. In this paper, a hysteresis model is presented which accurately captures the nonlinear behavior of reinforced concrete members in terms of a force-displacement, or moment-rotation, response. What makes this model attractive, when compared to other hysteresis models, is that unsymmetric sections (non-symmetric cross-section geometry and/or tension reinforcement amounts in the two loading directions), a cyclic axial load, and strength degradation may be included. The model is based on a few simple rules. Results based on the proposed hysteresis model show close agreement with various experiments on reinforced concrete members.

Keywords: bridge; damping; ductility; dynamic; hysteresis; nonlinear; practical design; reinforced concrete; seismic.

INTRODUCTION

Recent bridge failures caused by moderate to strong earthquakes in California and elsewhere have prompted a renewed interest in understanding the nonlinear seismic behavior of existing and new bridge structures. To accurately model the nonlinear dynamic response of a bridge structure subjected to a severe earthquake, an understanding of significant nonlinearities is required. Current bridge design philosophy dictates that inelastic behavior be strategically located at the ends of columns in the form of ductile plastic hinges. Based on capacity design principles, the adjacent superstructure and footings, as well as the column center portion, are protected against inelastic action by providing enough strength to force plastic hinges to form at the column ends. Therefore, a nonlinear dynamic time-history analysis of a typical bridge structure requires, among other things, that suitable nonlinear elements be used to accurately model the inelastic action expected at the column ends.

In the past, elasto-plastic hysteresis rules were frequently used to model the nonlinear behavior of columns. Although this model might prove reasonable for steel members, it is not a good representation of reinforced concrete. In 1970, Takeda et al. published a paper which included a set of general hysteresis rules for the response of reinforced concrete members, commonly called the Takeda Degrading Stiffness Model.[1] In this landmark paper, the importance of correctly modeling the cyclic behavior of reinforced concrete was demonstrated by excellent comparisons to dynamic response test results. It was shown that the constantly changing stiffness of reinforced concrete, producing less damping per cycle than an elasto-plastic response, must be explicitly accounted for in the hysteresis rules to produce realistic nonlinear dynamic results. In the years that followed this paper, changes were made to the basic model, resulting in the Modified Takeda Model.[2] The most notable difference is that the pre-cracked stiffness is often no longer included, resulting in an initial stiffness based on the cracked section. Time-history results using the cracked stiffness have been shown to agree very well with results using the original Takeda model.[3] Some form of the Modified Takeda Model is used in several nonlinear programs.[2,4]

The 1970 Takeda paper showed that a stiffness-degrading hysteresis model can adequately capture the nonlinear dynamic response of a reinforced concrete cantilever column subjected to base excitation. Not included in the Takeda Model are (1) variable column axial loads, (2) unsymmetric sections, (3) shifting of the column point-of-contraflexure, (4) biaxial bending effects, and (5) sudden strength degradation in non-ductile members and response modes.

Since the Takeda Model was introduced many other hysteresis models have been proposed, as discussed by Ghosh,[5] with varying levels of sophistication and capabilities. To include biaxial bending and varying axial loads, several hysteresis models (4 or 5) are typically used at the critical

ACI Structural Journal, V. 95, No. 5, September-October 1998.
Received March 27, 1997, and reviewed under Institute publication policies. Pertinent discussion will be published in the July-August 1999 *ACI Structural Journal* if received by March 1, 1999.

Robert K. Dowell is a senior engineer with ANATECH Corp. and a lecturer of structural engineering at the University of California, San Diego, where he received his MS degree. He has worked as a bridge engineer with Caltrans. His research interests include nonlinear seismic analysis and design of reinforced concrete structures.

ACI member Frieder Seible is a professor of structural engineering at the University of California, San Diego. He is a member of joint ACI-ASCE Committees 334, Concrete Shell Design and Construction, and 343, Concrete Bridge Design; and ACI Committees 341, Earthquake Resistant Concrete Bridges, and 437, Strength Evaluation of Existing Concrete Structures.

Edward L. Wilson is a Professor Emeritus of Structural Engineering at the University of California at Berkeley, where he was a faculty member from 1965 to 1991. He has been responsible for the development of several computer programs that are extensively used in the civil and mechanical engineering fields. He is currently chairman of the Engineering Criteria Board of BCDC and chairman of the Seismic Review Committee for the Berkeley campus.

section representing composite (concrete and steel) nonlinear springs.[6]

Some of the above-mentioned issues can be addressed by fiber or filament models, in which the member cross-section is divided into many longitudinal filaments representing the longitudinal steel, and confined and unconfined concrete. Cyclic stress-strain rules are assigned to each material, allowing the moment-curvature hysteresis response to be found, including variable axial load and members with any combination of materials, loading, and section shape. The force-displacement (or moment-rotation) response of the member is found by assuming a plastic hinge length, or by monitoring the moment-curvature response at several sections along the member length.

Recent efforts in fiber modeling, by Taucer et al.,[7] for example, show that good hysteresis results of reinforced concrete columns and beams are possible, when reasonable hysteretic constitutive assumptions for concrete and reinforcement filaments are used. The success of fiber modeling techniques has led some researchers to conclude that this approach is the most reasonable for the dynamic nonlinear analysis of bridge structures. However, the computational cost and storage requirements of even a single-degree-of-freedom fiber model can be prohibitive within the framework of a nonlinear time-history analysis. It is not reasonable to use this method at the ends of each column of an entire bridge structure for routine design and/or analysis. Therefore, predefined member end force deformation hysteresis models need to be developed which can accurately describe the inelastic response. Required parameters can be calibrated from the more advanced fiber model analysis and verified (where possible) from experimental results.

In this paper, a hysteresis model is presented for force-displacement or moment-rotation response of reinforced concrete members. Effects of a cyclic axial load, lack of section symmetry, and strength degradation are included. The use of the more advanced fiber model for calibration of the hysteresis parameters is demonstrated for circular columns and verified by experimental results. The primary advantage of the proposed hysteresis model, when compared to other models found in the literature,[5] is its ability to capture the dominant nonlinear characteristics of very complicated member response with three simple rules.

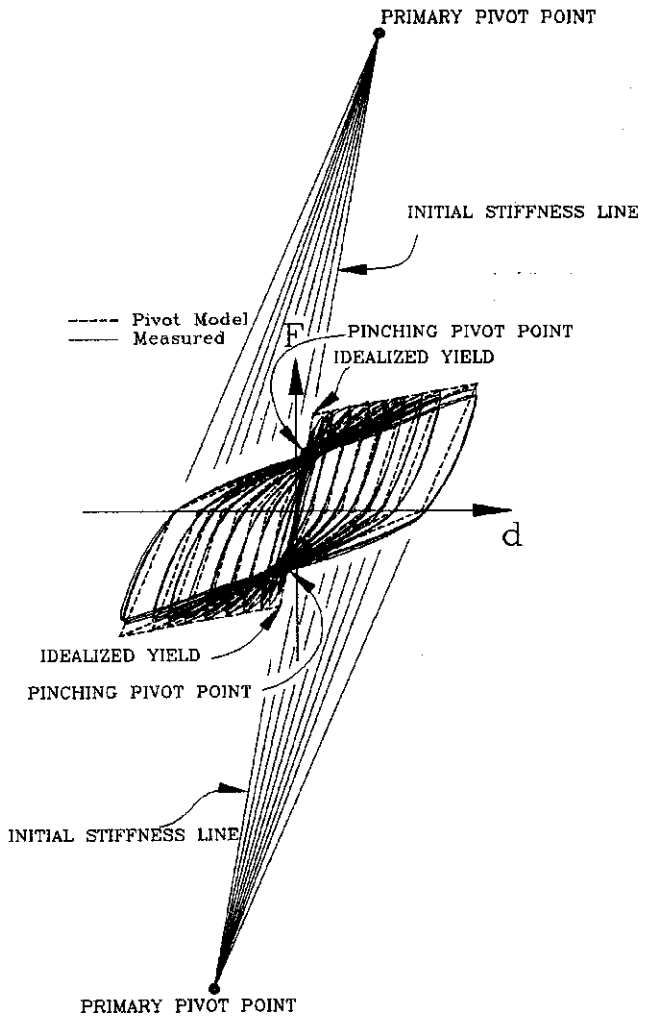

Fig. 1—Typical force-displacement behavior of reinforced concrete column

RESEARCH SIGNIFICANCE

This paper presents a new hysteresis model for the nonlinear response of reinforced concrete members. The cyclic behavior of the model follows three simple rules based on geometry. Despite its simplicity, the Pivot Model gives good results as judged by comparisons to measured results, and results from the more rational fiber model.

MODEL DEVELOPMENT

Measured force-displacement hysteresis results of large-scale reinforced concrete members[8] consistently show that (1) unloading stiffness decreases as displacement ductility increases, and (2) following a nonlinear excursion in one direction, upon load reversal, the force-displacement path crosses the idealized initial stiffness line prior to reaching the idealized yield force (unlike elasto-plastic response). Experimental observations show that unloading, back to zero force from any displacement level, is generally guided toward a single point in the force-displacement plane, on the idealized initial stiffness line (primary pivot point in Fig. 1). This is not a new idea; others have previously used the same approach for unloading.[9] Also observed is that all force-displacement paths tend to cross the elastic loading line at approximately

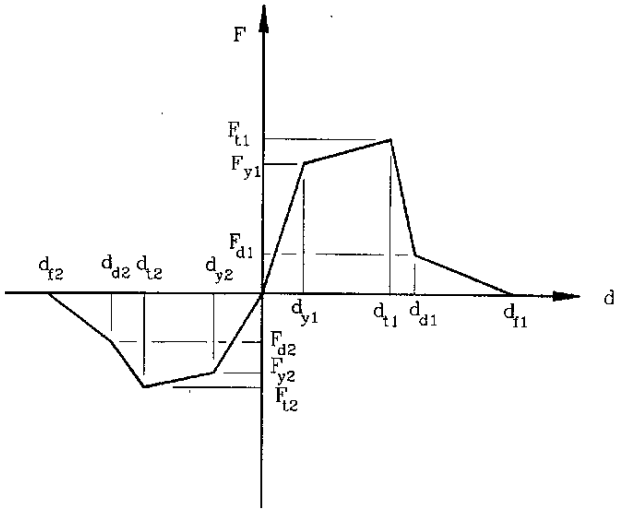

Fig. 2—Strength envelope

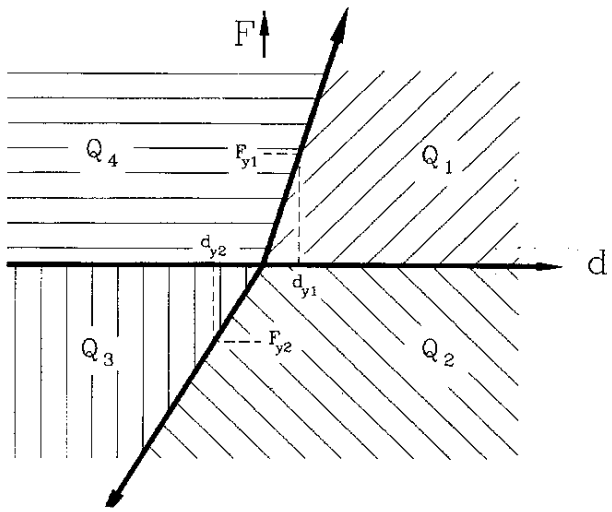

Fig. 3—Quadrant definition

the same point (pinching pivot point in Fig. 1). The development of the proposed model starts with these observations and expands them to a hysteresis model for very complex situations. Note that the force-deformation designation used in the Pivot Model description is completely general. It can represent the moment-rotation response of a plastic hinge, force-displacement response of a column in single or double bending, or force-displacement response of an entire bridge frame. Experimental results shown in Fig. 1 are for specimen C2 described later.

Description of rules

The Pivot Model is governed by a set of rules which depend on the properties of the member and the history of loading. Because the model must represent all possible loading sequences and member response paths, the rules must be complete and result in a unique force-deformation relationship. Figure 2 displays the strength envelope for monotonically increasing positive and negative loading, which is taken as the upper bound for cyclic loading, and may be determined as discussed in Ref. 10. The first and second branches of the strength envelope model elastic stiffness (cracked section) and strain-hardening stiffness, respectively. The third branch represents strength degradation, such as from shear failure, confinement failure, or bar pullout. The fourth, and final, branch allows for a linearly decreasing residual strength.

As demonstrated in Fig. 2, the two loading directions can have different strength envelopes. In this way, members which are unsymmetric, or have a cyclic axial load associated with frame action, may have different initial cracked stiffnesses (based on first yield of the reinforcement as discussed in Ref. 10) and yield forces (nominal member capacity) represented for the two loading directions. It should be noted that these properties may be found from a simple push-over analysis of the frame (based on the plastic capacity of the columns) when a cyclic axial load is considered and no strength degradation is included. The analysis indicates additional axial load in one loading direction, and reduced axial load in the opposite loading direction, with corresponding changes to the initial cracked stiffness and yield force of the member. In this way, a cyclic axial load is treated in the same fashion as an unsymmetric member, with the initial stiffness, yield force, and hysteretic parameters specified separately for the two directions of loading. Note that the cyclic axial load discussed in this paper is a consequence of frame action which allows the force-deformation envelope to be defined using a unique relationship between deformation and axial load. The more general variation in axial load associated with vertical accelerations is not included in the hysteretic response.

Prior to presenting rules which define unloading and reloading, it is necessary to define four quadrants, as shown in Fig. 3. Note that the four quadrants are defined by the horizontal axis and the elastic loading lines (not the vertical force axis), as indicated by the hatching in Fig. 3. This definition simplifies the model since different rules apply on either side of the elastic loading lines. It is also necessary to define primary pivot points P_1 through P_4, which control the amount of softening expected with increasing displacement, and pinching pivot points PP_2 and PP_4, which fix the degree of pinching following a load reversal (Fig. 4). As will become evident in the rules section discussed later, the number designation of the pivot points (Fig. 4) corresponds to the particular quadrant they affect. For example, unloading and loading in quadrant Q_1 is guided by point P_1. From Fig. 4 it is clear that the pivot points lie on the elastic loading line which corresponds to the quadrant they affect. This ensures that the complete force-displacement plane is covered for members with different initial (cracked) stiffnesses in the two directions of loading.

The response follows the strength envelope shown in Fig. 2 so long as no displacement reversal occurs. Once the yield deformation has been exceeded (in either direction), a subsequent strength envelope is developed requiring the introduction of points S_1 and S_2 which move along the strength envelope and are defined by the previous maximum displacements (see Fig. 4). The modified strength envelope

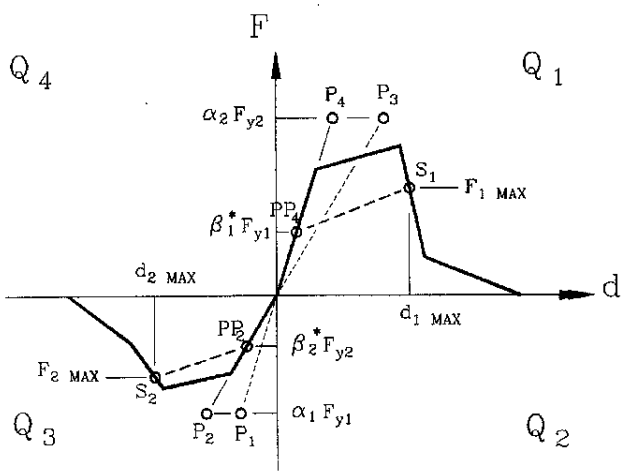

Fig. 4—Pivot point designations

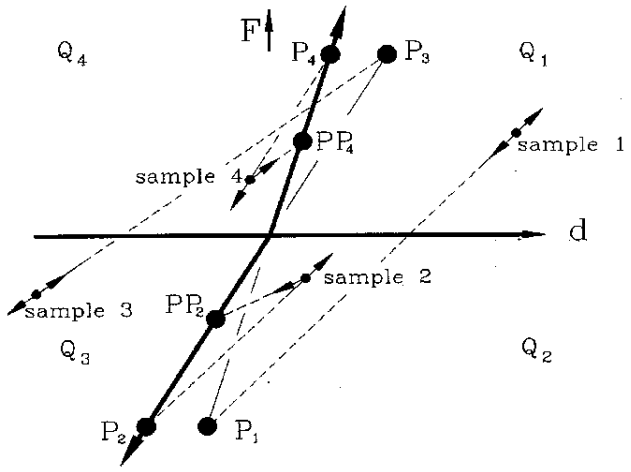

Fig. 5—Graphical representation of rules

(acting as the upper bound for future cyclic loading) is defined by lines joining points PP_4 to S_1, and points PP_2 to S_2 (Fig. 4). Although the pinching pivot points are initially fixed, they move toward the force-displacement origin once strength degradation has occurred. The parameters which define these points are

$$\beta_i^* = \beta_i \ (d_{iMAX} \leq d_{ti})$$

$$\beta_i^* = \frac{F_{iMAX}}{F_{ti}}\beta_i \ (d_{iMAX} > d_{ti})$$

where β_1 and β_2 define the degree of pinching for a ductile flexural response prior to strength degradation. Displacements d_{iMAX} (Fig. 4) and d_{ti} (Fig. 2) are the maximum displacement and strength degradation displacement, respectively, in the "i" direction of loading.

The following is a list of rules which define unloading and loading for the four quadrants shown in Fig. 3. Loading is defined as $+\Delta d$ for quadrants Q_1 and Q_4 and $-\Delta d$ for quadrants Q_2 and Q_3, with Δd defined as a displacement increment. Unloading is defined as $-\Delta d$ for quadrants Q_1 and Q_4, and $+\Delta d$ for quadrants Q_2 and Q_3. For the force-displacement path to leave the current strength envelope, a displacement reversal is required. While viewing these rules it may help to look at Fig. 5 which displays the same rules graphically. A sample point (in the force-displacement plane) is placed in each quadrant. The arrows extending from these sample points represent potential loading or unloading paths in the force-displacement plane.

RULES

Quadrant 1

- (Rule 1) Unloading—move along a line toward point P_1
- (Rule 2) Loading—move along a line away from point P_1

Quadrant 2

- (Rule 3) Unloading—move along a line away from point P_2
- (Rule 4) Loading—move along a line toward point PP_2

Quadrant 3

- (Rule 5) Unloading—move along a line toward point P_3
- (Rule 6) Loading—move along a line away from point P_3

Quadrant 4

- (Rule 7) Unloading—move along a line away from point P_4
- (Rule 8) Loading—move along a line toward point PP_4

By examining the list of rules above, the number of rules can be condensed to a set of three simple rules. This is due to the logical numbering which was assigned between pivot points and quadrants, allowing the use of symmetry to reduce the number of rules. The reduced set of rules is given below.

CONDENSED SET OF RULES

Quadrants 1 and 3

- (Rule 1) Loading and unloading in quadrant Q_n is directed away from or toward point P_n, respectively

Quadrants 2 and 4

- (Rule 2) Loading in quadrant Q_n is directed toward point PP_n
- (Rule 3) Unloading in quadrant Q_n is directed away from point P_n

Modified Pivot Model

The hysteresis model presented thus far does not recognize a softened initial stiffness following a nonlinear excursion. In other words, if the force-displacement path passes through the origin, the initial elastic stiffness is regained (until the modified strength envelope is encountered). However, experimental and fiber model results indicate a softened initial stiffness following a large nonlinear excursion. This is also seen in dynamic tests where the natural period of the structure is lengthened at the end of the experiment.

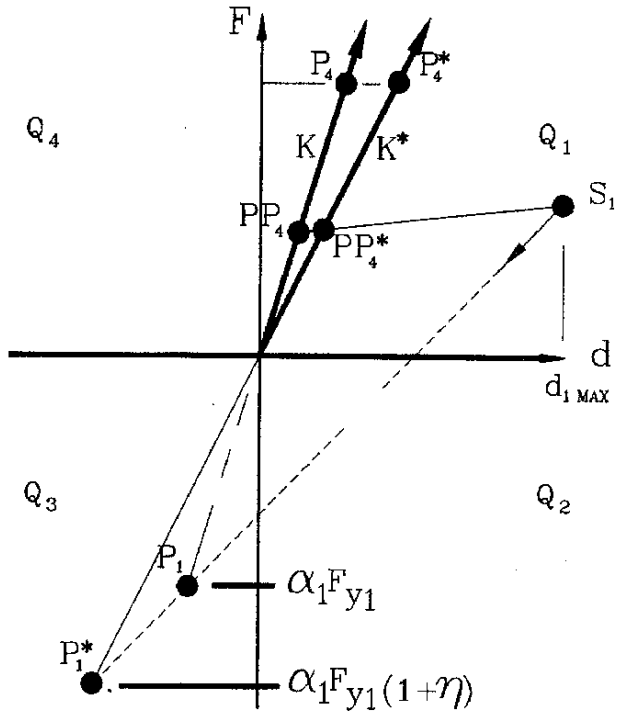

Fig. 6—Modified elastic loading line

To include this phenomenon within the framework of the Pivot Model, the elastic loading lines are free to rotate as a function of the maximum deformation and specified parameter η (Fig. 6). Therefore the quadrant definition is updated whenever the previous maximum displacement is exceeded in either direction. Figure 6 demonstrates the rotation of the elastic loading line adjacent to quadrants Q_1 and Q_4. The unloading stiffness of the maximum displacement excursion in quadrant Q_1 is guided toward point P_1 (unloading stiffness is same as original model at maximum displacement). This line continues until point P_1* is reached at a force $(1 + \eta)$ times larger than the force which defines point P_1. A line extending from point P_1* through the origin defines the new softened elastic loading line K*, and updated quadrants Q_1 and Q_4. Point P_4* is on the new elastic loading line at the same force level as point P_4. Point PP_4* is also on the new elastic loading line, but at a force defined by the intersection of the modified strength envelope (line between points PP_4 and S_1) and K* (Fig. 6). The hysteresis rules provided earlier are used with the updated pivot points (indicated by an asterisk).

The points in quadrants Q_1 and Q_4 are affected because they border the modified elastic loading line. The same procedure is followed if a nonlinear displacement occurs in the opposite loading direction, reducing the elastic loading line between quadrants Q_2 and Q_3, thus changing the behavior in those quadrants. Note that with $\eta = 0$, the model is identical to the original model. With a large value of η (say, 10) the unloading stiffness for small cycles is approximately equal to the unloading stiffness at maximum displacement. To the authors' knowledge this is the only hysteresis model capable of specifying the degree of initial stiffness loss.

PARAMETERS FOR CIRCULAR RC COLUMNS WITHOUT STRENGTH DEGRADATION

The required hysteresis parameters for symmetric sections with no axial load variation and without strength degradation are α and β (Fig. 4). Results from multiple analyses of circular reinforced concrete columns (Fig. 7) using a simplified fiber model,[11] indicate that these parameters may be expressed as a function of the longitudinal steel ratio and axial load ratio (axial load divided by the unconfined concrete strength and gross section area - $P/f'cAg$). Since the charts were developed with Grade 60 reinforcement, an effective longitudinal steel ratio of $^2/_3$ the actual ratio should be used for Grade 40 steel. The required bilinear envelope of the Pivot Model can be found from moment-curvature analysis.

Chart verification

To examine the validity of the charts presented in Fig. 7, parameters α and β are measured from experimental results of circular reinforced concrete column specimens C2, C4, G1, and F4 (as shown in Ref. 11). The parameters are taken as the average values from push and pull directions at displacement ductility 6. α is found at the intersection of the initial cracked stiffness and the softened unloading stiffness, defined by a line from the force at displacement ductility 6 through the displacement at zero force. β is found following a load reversal at the intersection of the force-displacement path and the initial cracked stiffness. Columns C2 and C4 are shear-critical columns[12] which were retrofitted to behave flexurally, while G1 is a flexural column[13] which will be discussed in greater detail later. F4 is also a flexural column.[8] Table 1 displays relevant information for each specimen, including measured hysteresis parameters α and β. By comparing these parameters with those obtained from Fig. 7 (and displayed in Table 1), the column tests indicate that the contours derived from the fiber model are realistic. Measured α parameters for Specimens C2, C4, and G1 are slightly lower than the chart values, while the measured α parameter for Specimen F4 is slightly higher. Pinching characteristics, rep-

Table 1—Specimen details and measured and calculated hysteresis parameters

Specimen	Axial load ratio, percent	Longitudinal steel ratio, percent	Effective longitudinal steel ratio, percent	α, measured	α, chart (Fig. 7)	β, measured	β, chart (Fig. 7)
C2	6	2.5	1.67	5	6	0.50	0.50
C4	18	2.5	1.67	1.5	1.8	0.35	0.52
G1	15	2.65	2.65	4	5	0.55	0.55
F4	18	2.5	1.67	2.3	1.8	0.45	0.52

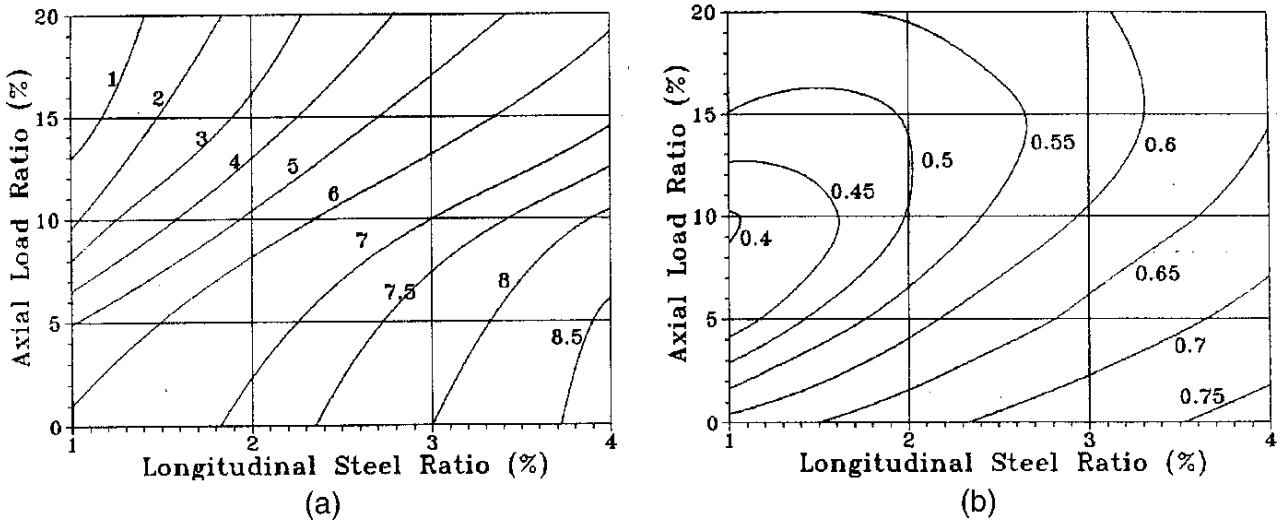

Fig. 7—Contours for hysteresis parameters for circular reinforced concrete columns: (a) α parameter, and (b) β parameter

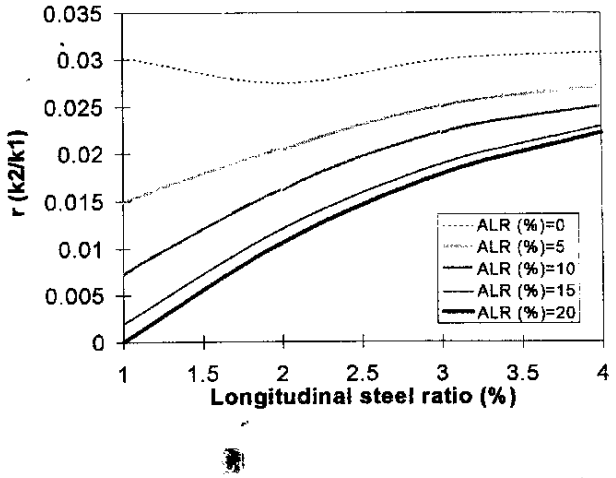

Fig. 8—Ratio of post-elastic stiffness to initial cracked stiffness "r" for circular columns

resented by β, are accurately captured for specimens C2 and G1, and are reasonably close for specimen F4. Specimen C4 showed more pinching than that predicted from the fiber model. This is probably due to the high shear forces of this column, which is known to cause pinching and reduction of β. Overall, measured parameters from the four specimens match those found from the chart (developed by fiber model analyses) very well.

In addition to the hysteresis parameters discussed above, the ratio of post-elastic stiffness to initial cracked stiffness "*r*" is provided in Fig. 8 as a function of the axial load ratio (ALR) and longitudinal steel ratio. This figure was also developed from fiber model analyses.

MODEL VERIFICATION

Loading in deformation control

To demonstrate the capabilities of the proposed model in deformation control, measured force-displacement hysteresis loops for circular reinforced concrete cantilever column specimen G1 (Fig. 9) are compared with results from the Pivot Model (modified, unloading stiffness of small displacements approximately equal to unloading stiffness at maximum displacement with $\eta = 10$). As a bench-mark, the Takeda model is included in some of the comparisons, as well as the more rigorous fiber model. Since it is not the purpose of this paper to discuss the test specimen in detail, only a cursory explanation is provided. Further details of the test specimen can be found elsewhere.[13] In the following figures the member force F is normalized to the nominal force F_n (force ratio) and the displacement is normalized to the idealized yield displacement (displacement ductility) permitting the hysteretic response of various members to be displayed in dimensionless form.

Column tests are typically conducted with increasing displacements in both loading directions, producing symmetric hysteresis loops. Although this loading provides valuable information, such as energy dissipation characteristics for a given ductility level, as well as the expected monotonic response, there are important hysteretic modeling considerations that remain unanswered. Under the influence of an earthquake, displacement cycles will differ greatly from artificially imposed, steadily increasing, symmetric loading cycles of the laboratory. For example, it is clear from typical reinforced concrete column tests that unloading stiffness softens as ductility is increased. What is not known from these experiments is how the member stiffness, at small ductilities, is affected by previous excursions to larger ductility levels. Also unanswered is the direction the force-displacement path takes if cycling occurs in one direction only.

Specimen G1 had its loading pattern intentionally altered from the standard fully reversed cyclic testing procedures of the laboratory[13] to ensure that the Pivot Model responds appropriately for a more realistic loading. Figure 10 shows that portion of the loading history which contain these added displacement cycles. With α and β found earlier from the charts as 5 and .55 (Table 1), and ratio of post-elastic stiffness to

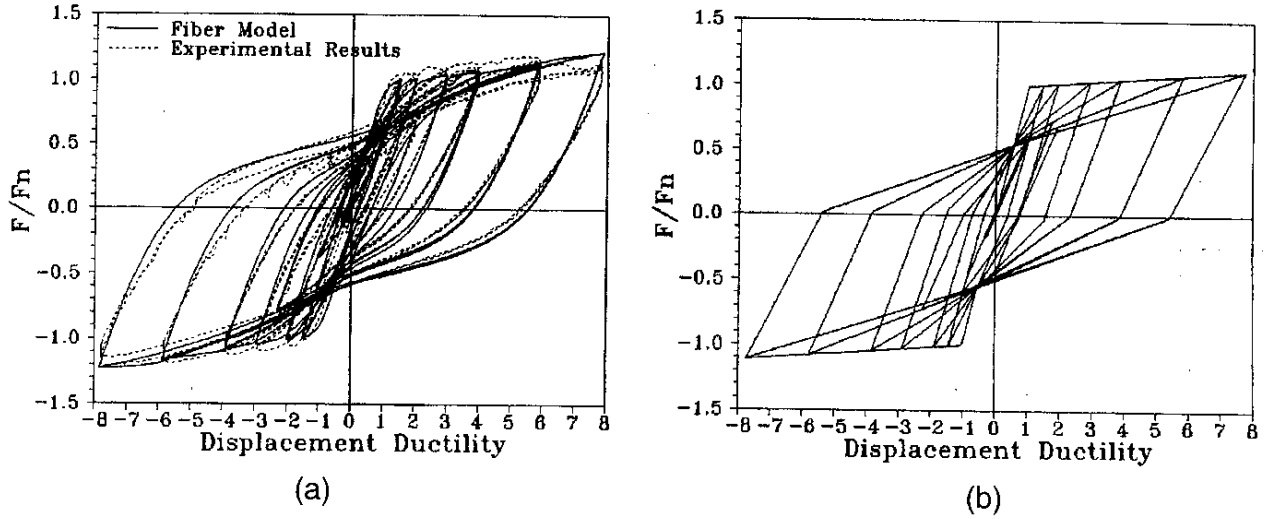

Fig. 9—Complete test of Specimen G1: (a) measured and fiber model results, and (b) Pivot Model results

initial cracked stiffness "r" of .01 (from Fig. 8), the Pivot Model responds similarly to the test specimen (Fig. 9).

Figure 11 compares measured unsymmetric force-displacement cycles, to the response of the Pivot Model, Takeda Model, and fiber model. Figures 11(b), (d), and (f) compare the measured response of an additional cycle applied in the same loading direction (corresponding to $^1/_2$ cycles 3 through 5 in Fig. 10), with results from the fiber, Pivot and Takeda models. Figures 11(a), (c), and (e) compare the measured response of small displacement cycles following large displacement cycles (corresponding to $^1/_2$ cycles 11 through 15 in Fig. 10), with results from the fiber, Pivot and Takeda models.

Figure 11 demonstrates that the response of the proposed hysteresis model closely resembles the measured response, while the Takeda Model tends to point to the previous maximum displacement too early, resulting in a response for unbalanced cycles which may be quite different from that measured. The measured amount of energy dissipated (relative energy in terms of ductility and force ratio) at each ductility level tested (Fig. 12[a]), is similar to that found from the Pivot Model and Modified Takeda Model (calibrated to match the unloading stiffness of the Pivot Model at displacement ductility 4). This shows that for the simple case of a symmetric member loaded with even displacement cycles, the Pivot Model behaves similarly to the widely used Takeda Model. Figure 12(b) indicates the relative energy dissipated for the unbalanced loops (loops 1, 2, and 3 correspond to $^1/_2$ cycles 11 through 15, neglecting the small inner loop, 3 through 5, and 12 through 14, respectively, in Fig. 10). As expected from Fig. 11, the energy dissipated from the Pivot Model is quite close to that measured, while the Takeda Model generally underestimates the energy dissipated. This is especially true for the larger unbalanced displacement cycle loop 1.

Dynamic loading

It was shown in the previous section that large symmetric displacement cycles and unbalanced displacement cycles of

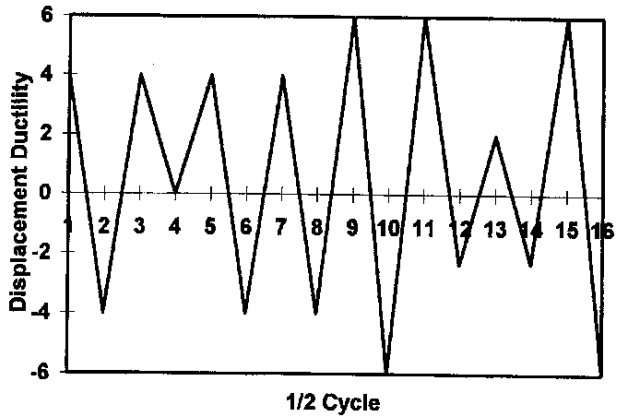

Fig. 10—Loading history for unbalanced cycles

a tested reinforced concrete column are well represented by the proposed Pivot Hysteresis Model. However, to more realistically test the rules of a hysteresis model it should be subjected to an earthquake motion. This exercises the force-displacement paths in somewhat random fashion, loading and unloading many times in each quadrant. As discussed previously, column specimen G1 was tested in deformation control. No dynamic loading of the specimen was conducted. However, a nonlinear time-history analysis of the specimen, subjected to the first 30 seconds of the 1940 El Centro earthquake (Imperial Valley Irrigation District, S00E), was performed with 2 percent viscous damping. The inertial mass is adjusted so that the initial elastic period of the structure is one second. In order to ensure reasonably large displacement ductility, the earthquake record is magnified by a factor of six over that required to produce the idealized yield force of the specimen (strength reduction factor Z of 6).

The same nonlinear analysis was conducted with the Pivot Model and the fiber model. The Modified Pivot Model was used, with unloading stiffness of small displacements ap-

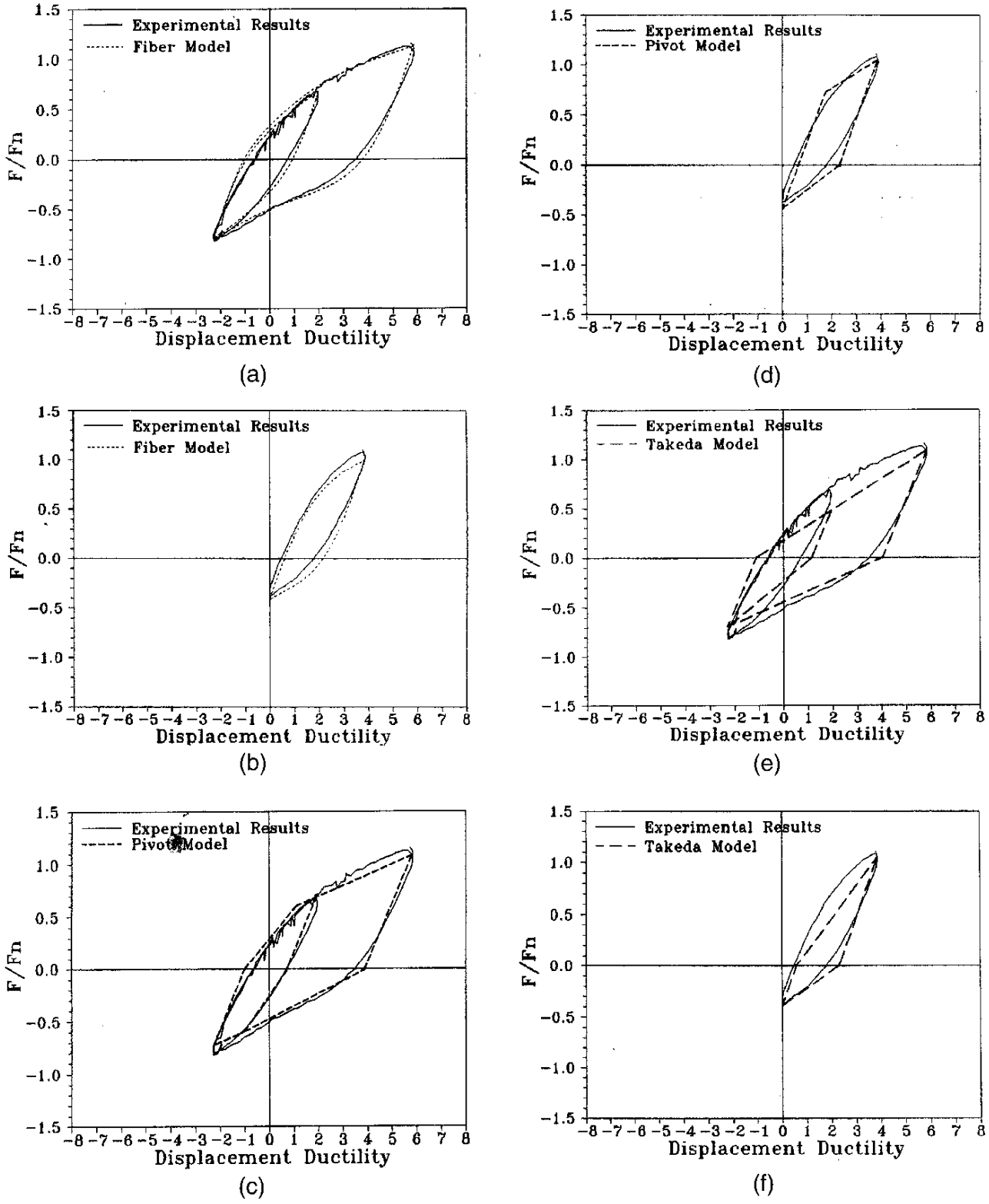

Fig. 11—Response of models compared to measured results for unbalanced displacement cycles of Specimen G1: (a) Loops 1 and 3 fiber model and measured; (b) Loop 2 fiber model and measured; (c) Loops 1 and 3 Pivot Model and measured; (d) Loop 2 Pivot Model and measured; (e) Loops 1 and 3 Takeda Model and measured; and (f) Loop 2 Takeda Model and measured

proximately equal to the unloading stiffness at maximum displacement ($\eta = 10$). This gave better results than the original Pivot Model following the maximum nonlinear excursion. As discussed previously, unlike a hysteresis model, the force-displacement response of a fiber model requires no rules. It is reasonable, therefore, to expect that the dynamic response of the fiber model will perform properly, and that it may be used as a bench-mark for the dynamic response of the

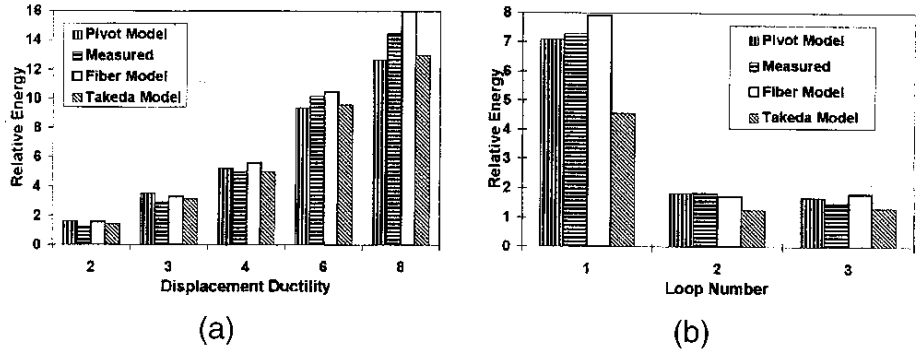

Fig. 12—Relative hysteresis energy: (a) symmetric displacement cycles, and (b) unbalanced displacement cycles

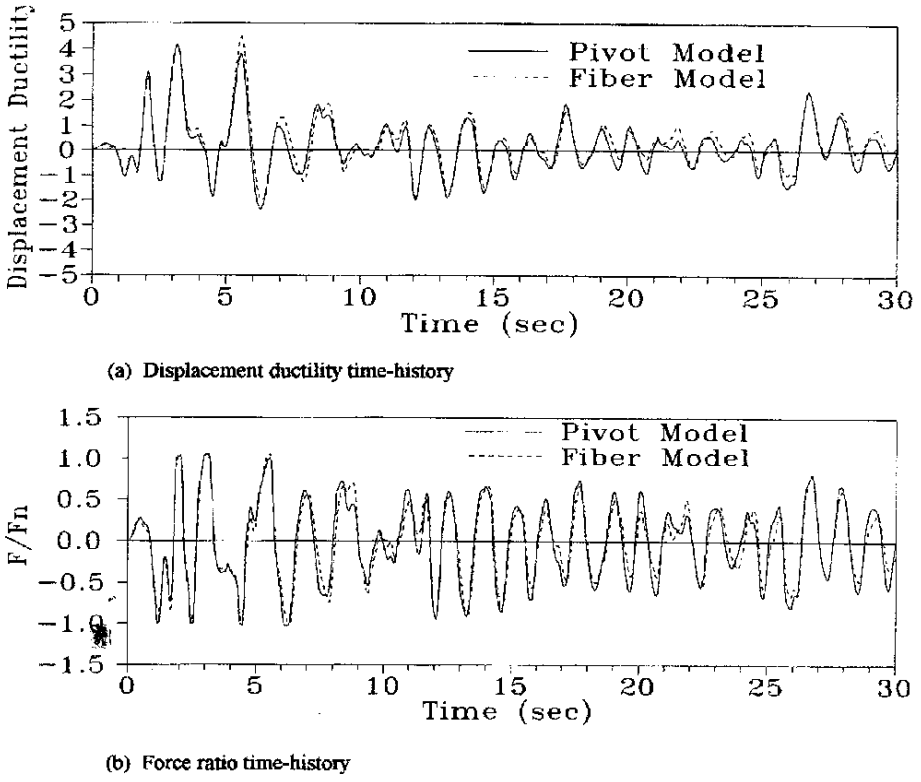

Fig. 13—Dynamic response of Specimen G1 subjected to the 1940 El Centro earthquake (constant axial load): (a) displacement ductility time-history, and (b) force ratio time-history

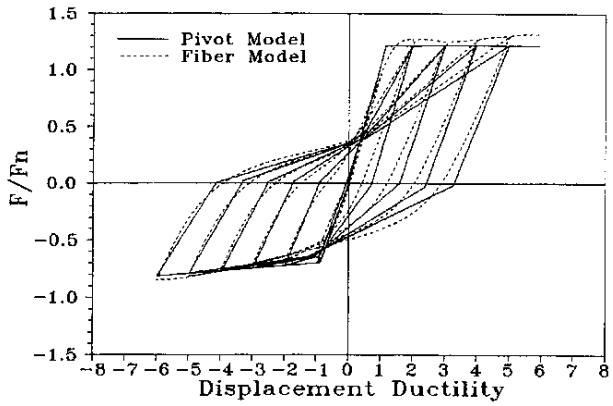

Fig. 14—Specimen G1 with varying axial load

Pivot Model. Figure 13 shows that the response of the Pivot Model is very similar to the fiber model behavior through the entire 30 seconds of loading. The displacement ductility time-history (Fig. 13[a]) indicates good correlation in maximum displacement and period of vibration. Also, force ratio time-history results show close agreement between the two models (Fig. 13[b]).

To demonstrate unsymmetric behavior of the proposed hysteresis model under dynamic response, specimen G1 is investigated with a cyclic axial load. The seismic axial load varies in proportion to the critical section moment with a constant of proportionality of 0.08 1/in. (0.0315 1/cm). Note that this constant was chosen arbitrarily to demonstrate unsymmetric member behavior associated with axial load variation which can be attributed to frame action. The fiber

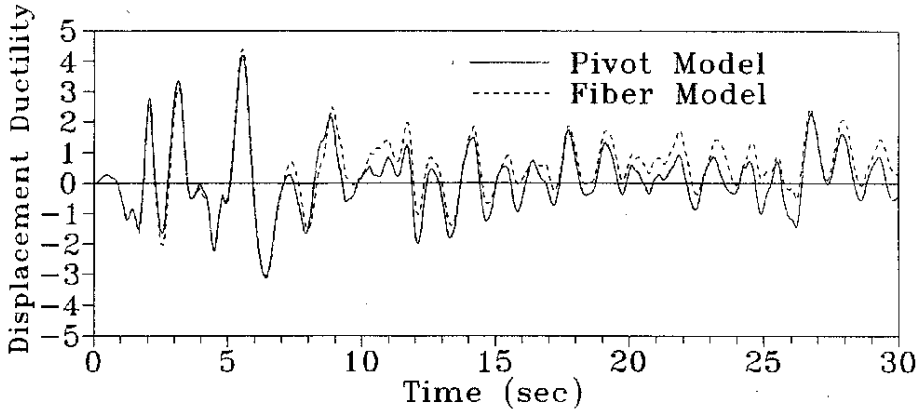

(a) Displacement ductility time-history

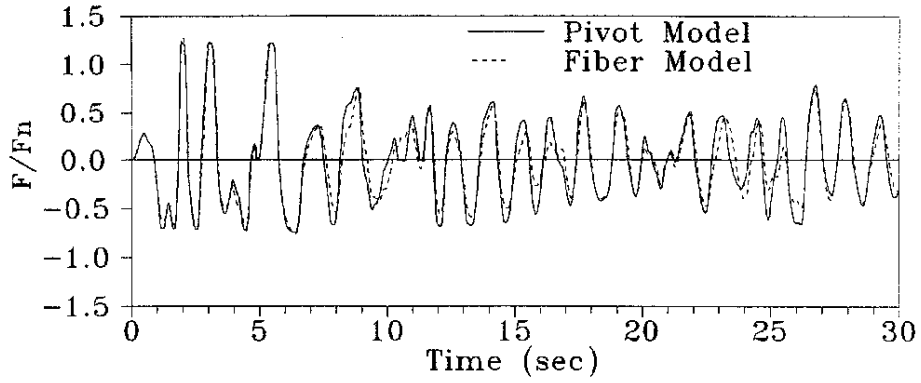

(b) Force ratio time-history

Fig. 15—Dynamic response of Specimen G1 subjected to the 1940 El Centro earthquake (varying axial load): (a) displacement ductility time-history, and (b) force ratio time-history

model response of the specimen in deformation control is shown in Fig. 14, along with the corresponding Pivot Model response. Required parameters of the Pivot Model were found from the fiber model results displayed in Fig. 14. In the following figures, nominal force and ductility one are based on dead load only, allowing response variations due to the changing axial load to be quickly observed. Figure 14 demonstrates that in deformation control the Pivot Model responds similarly to the fiber model with the large axial load variations induced.

As stated previously, a more thorough test of a hysteresis model is in its dynamic response. Therefore, specimen G1 was subjected to the first 30 seconds of the El Centro earthquake with the above discussed axial load variation, and magnification from the prior nonlinear analyses. A noticeable difference between the response of the specimen with axial load variation and without axial load variation is seen by viewing Fig. 13 and 15. The Pivot Model does a good job of mimicking the dynamic behavior of the fiber model (Fig. 15) for this unsymmetric column response. Figure 15(b) shows the importance of correctly modeling an unsymmetric response, with the force on the tension side being significantly less than nominal, and on the compression side much greater than nominal. This demonstrates that the proposed hysteresis model can quite accurately capture dynamic unsymmetric member behavior. Note that in this example a varying axial load caused the unsymmetric behavior. It could have been produced by other means, such as a different amount of reinforcement in the two loading directions, or an unsymmetric section shape.

OTHER POSSIBLE HYSTERESIS BEHAVIORS

The following provides several examples of possible Pivot Model behavior for various members and response modes. Unlike the previous examples, the Pivot Model parameters are taken directly from the measured data. Therefore these are not predictive models. Figures 16(a) and (b) show the response of a retrofitted outrigger bent, which performed in a ductile manner with no strength degradation, and an "as-built" outrigger bent, which failed in joint shear in one direction only.[14] Figure 16(c) demonstrates a classic column shear failure,[12] with sudden loss in force capacity prior to

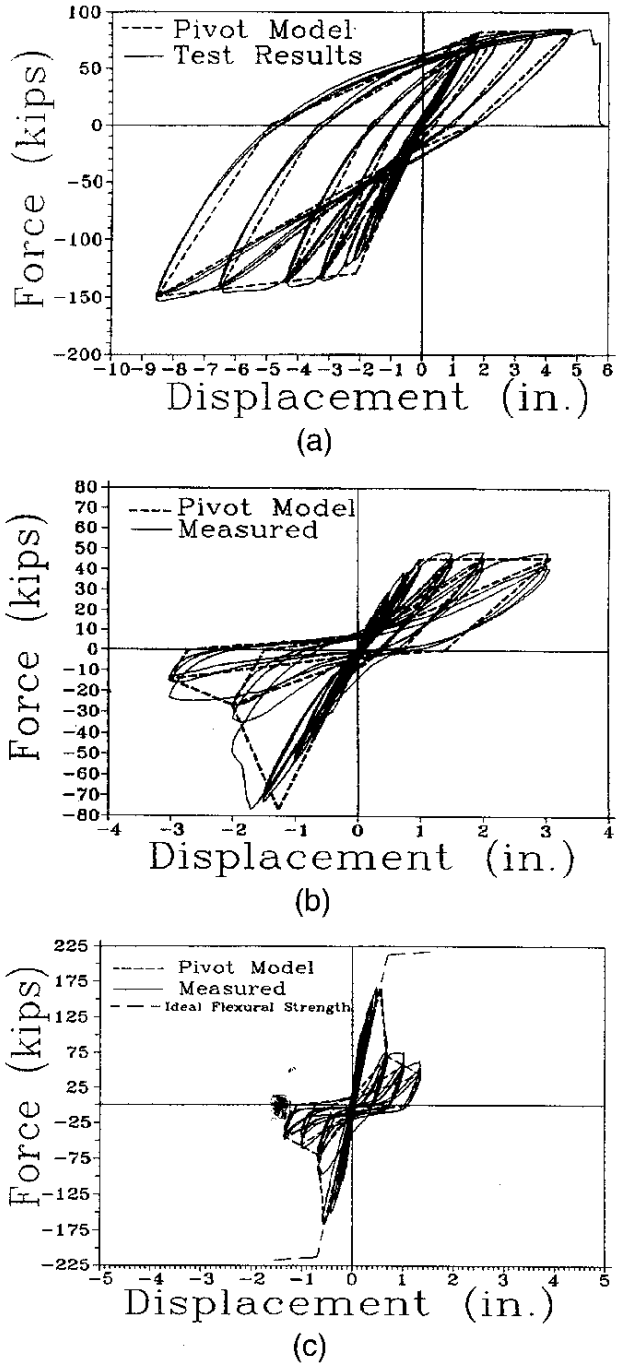

Fig. 16—Potential Pivot Model behavior compared with various experiments: (a) retrofitted knee joint (outrigger); (b) "as-built" knee joint (outrigger); and (c) shear column

ductility one. In all cases the proposed hysteresis model responds similarly to the measured results.

CONCLUSIONS

A simple and efficient hysteresis model is proposed for force-displacement, or moment-rotation, response of reinforced concrete members. For a symmetric column, with no strength degradation, the Pivot Model responds similarly to the popular Modified Takeda Model, with improved results for unsymmetric displacement cycles. It was shown that added effects from an unsymmetric section, cyclic axial load associated with frame action, and strength degradation may be included. Since strength envelope parameters, as well as unloading and loading parameters, are specified separately for the two loading directions, the hysteresis response can mimic very intricate behavior.

Presently, the Pivot Model does not include (1) continued strength degradation for multiple cycles to the same displacement level, (2) strength degradation in one loading direction caused by sudden strength loss in the opposite loading direction, and (3) biaxial bending effects. These phenomena are currently under investigation for inclusion in future versions of the Pivot Model. The unique quadrant approach of the Pivot Model, which is central to its hysteretic behavior, may aid in the development of a simple model which includes biaxial bending. To define the Pivot Model parameters and investigate the above discussed phenomena, a simplified fiber model is under development which closely matches experimentally obtained results.[11]

CONVERSION FACTORS

1 in. = 25.4 mm
1 kip = 4448 N

REFERENCES

1. Takeda, T.; Sozen, M. A.; and Nielsen, N. N., "Reinforced Concrete Response to Simulated Earthquakes," *J. Struct. Engrg. Div.*, ASCE, V. 96, No. 12, 1970, pp. 2257-2573.

2. Carr, A. J., *RUAUMOKO User's Guide*, Department of Civil Engineering, University of Canterbury, Christchurch, New Zealand, 1995.

3. Saiidi, M., "Hysteresis Models for Reinforced Concrete," *J. Struct. Engrg. Div.*, ASCE, V. 108, No. 5, 1982, pp. 1077-1087.

4. Powell, G. H., "Supplement to Computer Program DRAIN-2D," Supplement to Report, *DRAIN-2D User's Guide*, University of California, Berkeley, 1975.

5. Ghosh, S. K., *Earthquake-Resistant Concrete Structures Inelastic Response and Design*, ACI SP-127, American Concrete Institute, Detroit, 1991.

6. Jiang, Y., and Saiidi, M., "Four-Spring Element for Cyclic Response R/C Columns," *J. Struct. Engrg. Div.*, ASCE, V. 116, No. 4, 1990, pp. 1018-1029.

7. Taucer, F.; Spacone, E.; and Filippou, F. C., "A Fiber Beam-Column Element for Seismic Analysis of Reinforced Concrete Structures," *Report* No. UCB/EERC-91/17, College of Engineering, University of California, Berkeley, 1991.

8. Priestley, M. J. N., and Seible, F., "Seismic Assessment and Retrofit of Bridges," *Report* No. SSRP-91/03, Department of Applied Mechanics and Engineering Sciences, University of California, San Diego, 1991.

9. Kunnath, S. K.; Reinhorn, A. M.; and Park, Y. J., "Analytical Modeling of Inelastic Seismic Response of R/C Structures," *J. Struct. Engrg. Div.*, ASCE, V. 116, No. 4, 1990, pp. 996-1017.

10. Priestley, M. J. N.; Seible, F.; and Calvi, G. M., *Seismic Design and Retrofit of Bridges*, John Wiley and Sons, New York, 1996.

11. Dowell, R. K., "Nonlinear Seismic Analysis and Design of Reinforced Concrete Bridge Structures," PhD dissertation, University of California, San Diego, 1998.

12. Priestley, M. J. N.; Seible, F.; Xiao, Y.; and Verma, R., "Steel Jacket Retrofitting of Reinforced Concrete Bridge Columns for Enhanced Shear Strength–Part 2: Test Results and Comparison with Theory," *ACI Structural Journal*, V. 91, No. 5, Sept.-Oct. 1994, pp. 537-551.

13. Smith, G., "Strategic Relocation of Plastic Hinges in Bridge Columns," Master's Thesis, University of California, San Diego, 1996.

14. Ingham, J., "Seismic Performance of Bridge Knee Joints," Ph.D. Dissertation, University of California, San Diego, 1995.

ACI Structural Research Award

presented to:

Edward L. Wilson

2000

"for your co-authored paper, 'Pivot Hysteresis Model for Reinforced Concrete Members,' September/October 1998 ACI Structural Journal, which describes the development of a simplified approach for modeling the nonlinear behavior of reinforced concrete bridge structures subjected to earthquakes"

aci international

american concrete institute

President Jo Coke

Presentation Date March 30, 2000